The final publication is available at

Additional Information

In Silico Ischemia-Induced Reentry at the Purkinje-Ventricle Interface

Esteban Ramírez[1], Javier Sáiz[2], Lucía Romero[2], José M. Ferrero Jr.[2], and Beatriz Trénor[2]

[1]Laboratorio de Bioingeniería, Departamento de Ingeniería Eléctrica y Electrónica, Instituto Tecnológico de Cuautla, Morelos, Mexico.

[2]Instituto Interuniversitario de Investigación en Bioingeniería y Tecnología Orientada al Ser Humano (i3BH), Universitat Politècnica de València, Valencia, Spain.

Address for proofs and correspondence:

Ph.D. Beatriz Trénor Gomis

Ciudad Politécnica de la Innovación

Cubo Azul Edif. 8B Acceso N

Camino de Vera s/n, 46022

Valencia (Spain)

Tel: +34 96 387 75 18

Fax: +34 96 387 76 09

E-mail: btrenor@gbio.i3bh.es

Abstract

Aims. This computational modeling work illustrates the influence of hyperkalemia and electrical uncoupling induced by defined ischemia on action potential (AP) propagation and the incidence of reentry at the Purkinje-ventricle interface in mammalian hearts.

Methods. Unidimensional and bidimensional models of the Purkinje-ventricle subsystem, including ischemic conditions (defined as phase 1B) in the ventricle and an ischemic border zone, were developed by altering several important electrophysiological parameters of the Luo-Rudy AP model of the ventricular myocyte. Purkinje electrical activity was modeled using the equations of DiFrancesco and Noble.

Results. Our study suggests that an extracellular potassium concentration $[K^+]_o$ greater than 14 mM and a slight decrease in intercellular coupling induced by ischemia in ventricle can cause conduction block from Purkinje to ventricle. Under these conditions, propagation from ventricle to Purkinje is possible. Thus, unidirectional block (UDB) and reentry can result. When conditions of UDB are met, retrograde propagation with a long delay (320 ms) may re-excite Purkinje cells, and give rise to a reentrant pathway. This induced reentry may be the origin of arrhythmias observed in phase 1B ischemia.

Conclusions. In a defined setting of ischemia (phase 1B) a small amount of uncoupling between ventricular cells, as well as between Purkinje and ventricular tissue, may induce UDBs and reentry. Hyperkalemia is also confirmed to be an important factor in the genesis of reentrant rhythms, since it regulates the range of coupling in which UDBs may be induced.

Keywords - Arrhythmias, phase 1B ischemia, intercellular coupling, computer simulations, reentry, hyperkalemia.

Condensed abstract

This computational work, in the setting of phase 1B ischemia, reveals that even minimal uncoupling within the Purkinje-ventricle subsystem may induce unidirectional block. In contrast, a more extensive uncoupling facilitates AP propagation. Hyperkalemia also represents an important modulating factor since $[K^+]_o$ regulates the range of coupling in which reentry may be induced.

What's New?

New theoretical models have been developed to simulate the electrophysiological changes arising in the Purkinje-ventricle interface during phase 1B ischemia. Novel insights from the work include:

(i)   The probabilities of unidirectional block and reentry increase in the presence of a low degree of uncoupling within the endocardium, and/or between Purkinje and ventricular fibers.

(ii)   An intermediate degree of this uncoupling may preserve conduction, thus avoiding the emergence of reentrant circuits.

(iii)   A high degree of uncoupling results in the substrate showing bidirectional block and no reentry may be generated.

(iv)   The amount of hyperkalemia during ischemia (phase 1B) is a major factor in the generation of conduction block.

(v)   Reentrant pathways in the Purkinje-ventricle subsystem can arise as a consequence of phase 1B ischemia and arrhythmias result.

Introduction

Regional myocardial ischemic episodes are closely related to cardiac arrhythmias.[1] The arrhythmias induced by ischemia have been categorized into distinct phases and each may have different mechanisms.[2] Experimental studies carried out on canine hearts have shown that arrhythmias during phase 1A often arise in the interval from 2-8 minutes after the onset of myocardial ischemia.[3] Thereafter, a second phase (denoted 1B) of rhythm disturbances has been well characterized.[3-5]

The mechanisms for these arrhythmias are thought to be intimately related to the electrophysiological changes during phase 1B of ischemia. These include cellular uncoupling,[4,6] an increase of extracellular potassium $[K^+]_o$,[4,7,8] reductions in catecholamine levels,[9] and left ventricular wall stress.[10]

Experimental studies have established a relationship between ischemia-induced arrhythmias during phase 1B, and the increase in impedance of ventricular tissue (R_t), occurring approximately 13 to 15 minutes postocclusion.[4,8] The time-course of these increases in R_t and $[K^+]_o$,[11,12] and their extent vary considerably. Nonetheless the degree of hyperkalemia and endocardial uncoupling are determinants of arrhythmias in the phase 1B of ischemia.

The Purkinje network is essential for action potential (AP) propagation and ventricular contraction in mammalian hearts. The uncoupling induced by ischemia at the Purkinje-ventricle interface and the ischemic endocardium contribute to arrhythmogenesis.

The main objective of the present work was to evaluate the influence of conditions of 1B ischemia on AP conduction between Purkinje system and ventricular tissue, and reveal the role of these factors in reentry.

Methods

A. Action Potential Models

To simulate the electrical activity of the Purkinje-ventricle subsystem, well-characterized AP models based on Hodgkin-Huxley formulation were used. Specifically, a modified version of the Luo-Rudy phase II model (LRd00)[13,14] was used to reproduce the electrophysiological characteristics of endocardial ventricular myocytes under normal and 1B ischemia conditions. The formulation of Ferrero and coworkers of the ATP-sensitive potassium current ($I_{K(ATP)}$), which reproduces with fidelity ischemic changes,[15-18] was also included in the LRd00 model.

A number of models for the Purkinje fiber AP have been published for rabbit,[19,20] dog,[21,22] mouse,[23] and human.[24] A detailed comparison of these models can be found in reference 22. In the present work, the AP of Purkinje cells was simulated using a modified version of DiFrancesco-Noble model.[25] The maximum conductance of the sodium current (g_{Na}) was changed from 750 to1125 µS to achieve a value of the maximal AP upstroke velocity that lies within the known range under control conditions.[26]

B. Model of Phase 1B of Ischemia

Several parameters in the LRd00 model were modified as in Pollard et al.[27] to simulate the electrophysiological changes of ventricular cells during the period 15 to 45 minutes after the onset of ischemia. Some of the parameters were changed with respect to Pollard et al. model[27] and were chosen from experimental observations,[7,8] and simulation studies.[28] Details of these changes are in table 1.

In addition, ischemia-induced alterations in $[ADP]_i$ and R_{endo} were also evaluated. $[ADP]_i$ was set to 110 µM and R_{endo} was varied in the range 5 to 40 $\Omega \cdot cm^2$.[3,4,6] The ischemic ventricular trabeculum and tissue models were both divided into three zones: a central ischemic zone (CIZ1B), a border zone (BZ) and a normal zone (NZ). The parameters altered during phase 1B ischemia were varied in the BZ according to linear spatial gradients. A BZ of 1 cm in length was based on experimental observations.[29,30] The linear variations in the BZ were

present along 10, 5, and 1 mm of the tissue to simulate the effects of hyperkalemia, acidosis, and hypoxia, respectively.[30,31]

C. Tissue Models

In the present work several tissue models were developed. Firstly, in order to study the characteristics of AP propagation from Purkinje to ventricle and from ventricle to Purkinje, two 1D models were developed and consisted of a Purkinje fiber coupled to either a normal ventricular fiber (see Figure 1A) or a ventricular fiber affected by 1B ischemic conditions including a CIZ1B, a BZ and a NZ (see Figure 1B). In both models the Purkinje and ventricular fibers were coupled through a Purkinje-ventricle junction (PVJ). The delay in conduction associated to the PVJ was determined by the values of the Purkinje-ventricle resistance (R_{PVJ}). Under normal conditions, R_{PVJ} was adjusted to 16 $\Omega \cdot cm^2$, which resulted in a delay in conduction from Purkinje to ventricle of 2.21 ms. R_{PVJ} value was increased up to 40 $\Omega \cdot cm^2$ to simulate the effects of ischemia.[32,33] Purkinje and ventricular fibers were 1.5 cm (100 cells) and 3 cm (300 cells) in length, respectively. The stimulation protocol consisted of a train of 11 pulses applied at cell #0 of the Purkinje fiber in the two models. In the case of the Purkinje fiber coupled to the ischemic strand, the stimuli were also applied to the NZ of the ventricular end, to analyze the AP propagation from ventricle to Purkinje.

Secondly, a 1D model was defined with a ring structure, where a Purkinje fiber was coupled to an 1B ischemic ventricular strand through two Purkinje-ventricular junctions (PVJs). The Purkinje fiber was composed by 600 cells (9 cm) and the ventricular strand had 500 cells (5 cm). The ventricular fiber was divided into 300 cells in the CIZ1B, 100 cells in the BZ, and 100 cells in the NZ. Uncoupling in the PVJ in the ischemic zone was varied and quantified by an elevated value of R_{PVJ1}, whereas PVJ in the normal zone was characterized by normal coupling (R_{PVJ2}=16 $\Omega \cdot cm^2$).

The stimulation protocol consisted of two depolarizing pulses applied to cell #99 of the Purkinje fiber at a BCL of 1500 ms (see Figure 2).

A 2D model of a bundle of Purkinje cells coupled to ischemic ventricular tissue through Purkinje-ventricle junctions: PVJ1 in the ischemic zone and PVJ2 in the normal zone (see Figure 3). The bundle of Purkinje cells consisted of 5×452 nodes. The ventricular tissue had an anisotropy ratio of 3:1 and was composed by 275×250 nodes. Each node represented a membrane patch with dimensions 100×100 µm. The stimulation protocol consisted of one pulse applied at the site indicated in Figure 3.

D. Computation of the Safety Factor

The safety factor (SF) for conduction was computed and used to evaluate the AP conduction from Purkinje to ventricle and from ventricle to Purkinje. SF quantifies the source-sink relationship between adjacent cardiac cells. The value of the SF illustrates the success (SF value greater than 1) or failure (SF values lower than 1) of AP propagation. Several definitions of the SF have been published.[34-36] The formulation of Romero et al. (SF_R), was chosen based on its computational advantages.[37]

Results

A. Effects of 1B Ischemia on Cellular Electrophysiology

The electrophysiological changes in the setting of phase 1B ischemia were analyzed in the 1D ischemic fiber. APD_{90}, conduction velocity (CV) and resting potential (V_{rest}) were significantly changed. Specifically, APD_{90} was reduced by 70% in the CIZ1B for $[K^+]_o = 9$ mM, V_{rest} was -84 mV in the NZ and -64 mV in the CIZ1B when $[K^+]_o$ was 12 mM. CV was also reduced within the CIZ1B, especially when $[K^+]_o \geq 9$ mM.

B. Conduction Safety at the Purkinje-Ventricle Interface

The ischemia-induced alterations in the ventricular electrophysiology can affect AP propagation between the Purkinje system and ventricular tissue. To analyze the safety of AP conduction from Purkinje to ventricle (and from ventricle to Purkinje) we used the parameter SF described in the Methods section. Figure 1-A shows the safety factor calculated in a

Purkinje fiber coupled to a ventricular fiber under normal conditions. SF_R values were 2.5 and 1.82 in Purkinje and ventricular fibers, respectively.

SF_R was also evaluated in the 1D model of a Purkinje fiber coupled to a ventricular fiber under phase 1B ischemic conditions. Figures 1-B and 1-C depict the SF_R plots obtained for these two sets of simulations including selected degrees of coupling between Purkinje and ventricular fibers (R_{PVJ} = 16 and 24 $\Omega \cdot cm^2$). SF_R showed a biphasic behavior, as cellular coupling between ventricular cells decreased. This effect was observed for the cases illustrated in panels B and C. As depicted in Figure1-B, where R_{PVJ} and $[K^+]_o$ were set to 16 $\Omega \cdot cm^2$ and 11.5 mM, respectively, successful AP propagation was observed for low and moderate values of cellular uncoupling of ventricular cells (when R_{endo} was varied from 5 to 38 $\Omega \cdot cm^2$). More extensive uncoupling resulted in conduction block. Note that SF_R remained almost constant in the CIZ1B and its value depended on ventricular coupling. In contrast, SF_R in the BZ was ad a bell-shaped, as expected since conditions of simulated phase 1B ischemia were varied along the BZ. More extensive uncoupling between Purkinje and ventricular fibers (R_{PVJ} = 24 $\Omega \cdot cm^2$) also resulted in a biphasic behavior of the SF_R (see Figure 1C). SF_R dropped below unity and AP propagation failed at the CIZ1B for low and very high values of ventricular uncoupling.

Retrograde propagation from ventricle to Purkinje was also analyzed in our simulations by stimulating cell #399 of the ventricular fiber. A set of simulations was conducted for selected values of R_{endo}, $[K^+]_o$, and Purkinje-ventricle coupling (R_{PVJ}). The stimuli were applied either at the Purkinje or at the ventricular edge. Figure 1 panels D, E, and F show the results obtained. Three different patterns of results were observed: (i) AP conduction success from Purkinje to ventricle and from ventricle to Purkinje (white area), (ii) conduction block in both directions, i.e. bidirectional block (BDB) at the CIZ1B (light green area), and (iii) unidirectional block (UDB) at the PVJ or at the CIZ1B zone (dark green area). In the case of UDB, conduction block occurred from Purkinje to ventricle, whereas conduction was achieved from ventricle to Purkinje. This conduction block occurred in the ischemic ventricular cells, very close to the PVJ. More extensive uncoupling between Purkinje and ventricular fibers,

resulted in an increased probability of UDB (panel F). It is known that UDBs can set the stage for reentry in an ischemic tissue.[16-18]

C. 1B Ischemia-Induced Reentry

To investigate whether the UDBs identified in the 1D Purkinje-ischemic ventricle model can in fact generate reentry, simulations were conducted using a 1D model ring structure. Figure 2 shows the three scenarios described above: UDB and reentry (panel A), bidirectional conduction and AP collision (panel B), and BDB block at the CIZ1B zone (panel C), depending on the degree of cellular uncoupling of ventricular cells. In these simulations $[K^+]_o$ was set to 11.7 mM. R_{PVJ1} and R_{PVJ2} were set to 32 and 16 $\Omega \cdot cm^2$, respectively, to simulate the increased uncoupling in the ischemic region and the normal coupling in the normal region. Note that R_{endo} values differ in panels A, B, and C. The three selected cases are indicated by the crosses in Figure 1C. Figure 2A represents the first scenario, where 1B ischemic conditions led to UDB at PVJ1. In this case, R_{endo} was set to 9 $\Omega \cdot cm^2$. The wavefronts generated by the second pulse started to propagate in both directions along the Purkinje fiber. One of the wavefronts was blocked in the ventricular cells next to PVJ1. The second wavefront propagated through PVJ2, crossing the junction and starting its propagation along the normal zone of the ventricular fiber. When this second wavefront reached PVJ1 and propagation succeeded, Purkinje cells close to PVJ1 generated an AP and the new cycle of the reentry. This reentry was sustained until the end of the simulation (2600 ms).

When R_{endo} was increased to 10 $\Omega \cdot cm^2$, conduction block from Purkinje to ventricle disappeared (Figure 2B). In this case, the moderate uncoupling between ventricular cells modified the source-sink relationship between Purkinje and ventricular fibers, such that propagation was favored.

A further increase in ventricular uncoupling (R_{endo} = 25 $\Omega \cdot cm^2$) led to BDB at the CIZ1B (see Figure 2C). After propagating through the two PVJs (PVJ1 and PVJ2), BDB occurred at the CIZ1B due to high intercellular resistance: the two wavefronts failed to propagate. Our

simulations show that 1B ischemia may set the conditions that generate a reentry in the Purkinje-ventricle subsystem. Note however, that moderate uncoupling of ventricular cells, can favor conduction, prevent a reentry, and thus be antiarrhythmic.

Finally, we evaluated whether the reentry observed in the ring model can occur in a more realistic structure. For this purpose, we implemented a 2D model of a bundle of Purkinje fibers connected to ventricular tissue, as described in Methods. Figure 3 shows model output for two selected sets of conditions.

A single stimulus was applied at cell #0 of the Purkinje fiber (Figure 3A) and phase 1B ischemic parameters were set: R_{PVJ1} = 25.6 $\Omega \cdot cm^2$ (corresponding to an increased uncoupling in the ischemic junction), R_{PVJ2} = 16 $\Omega \cdot cm^2$ (corresponding to the normal coupling in the normal junction), R_{endo}=8 $\Omega \cdot cm^2$ and $[K^+]_o$ = 14.3 mM. Note that these values are different from those utilized in the 1D and ring models, since in 2D simulations the parameters yielding conduction block differ somewhat.

Under these conditions conduction block occurred at PVJ1 and the first wavefront could not propagate through the CIZ1B zone of the ventricular tissue. The second wavefront propagated through PVJ2, through the three ventricular zones, and reached PVJ1. Note that the wavefront failed to re-excite the Purkinje cells near PVJ1 and disappeared (panel A6 of Figure 3). A further increase in $[K^+]_o$ up to 14.5 mM led to reentry in the Purkinje-ventricle system, as illustrated in Figure 3B. In this case, one of the wavefronts failed to propagate across PVJ1, as in the previous case. However, the second wavefront did propagate across PVJ2, throughout the ventricular tissue, and later across PVJ1. This wavefront re-excited Purkinje cells, thus generating reentry. The time required for the second wavefront to reexcite Purkinje cells was 320 ms. These results suggest that even small changes in specific parameters characteristic of phase 1B ischemia can be critical in the generation of reentry.

Discussion

A. Electrical Uncoupling Induced by Phase 1B Ischemia

Several experimental studies have shown that during ischemia the impedance of the ventricular tissue increases between 40% and 200%.[4,33,38-40] This increase of tissue resistance appears to be connected with the incidence of arrhythmias.[38] The range of ventricular uncoupling (parameter R_{endo} was increased up to 80%) in which we observed UDBs, is within the range of the published data.

Details of the electrical uncoupling and conduction delay between Purkinje fibers and ventricular ischemic tissue are available from experimental studies.[33] However, the exact amount of uncoupling at PVJ induced by ischemia is unknown. Accordingly, we evaluated a maximum increase of 100% in the ischemia simulations (parameter R_{PVJ}), with respect to normal conditions.

B. Biphasic Behavior of the Safety Factor for Conduction

Our simulations show that the electrophysiological alterations induced by phase 1B ischemia change the SF_R in a biphasic manner. An intermediate increase in endocardial uncoupling led to a SF_R increase in the CIZ1B (see Figure 1), whereas CV was decreased, which is in accordance with previous theoretical studies. Indeed, Shaw and Rudy obtained an increase in SF and a decrease in CV when the conductance of gap junctions was reduced.[36] Dhein suggested that complete gap junction uncoupling would promote arrhythmogenesis, whereas an intermediate uncoupling would increase SF.[41] This conclusion is supported by other experimental studies in which the maximum ventricular uncoupling related to phase 1B of ischemia was 200% and a greater uncoupling was considered as complete uncoupling, which was related to the end of incidence of 1B phase arrhythmias.[4,6]

The biphasic behavior of SF_R results from the complex interaction of the modified electrophysiological parameters as a result of 1B ischemia. Cellular uncoupling together with hyperkalemia are both important factors. A progressive increase in $[K^+]_o$ led to a narrower

range of conduction (see white areas in Figure 1). It is noteworthy that in the Purkinje-1B ischemic ventricle model conduction block was obtained for $[K^+]_o$ greater than 11.7 mM. In a multicellular fiber model of 160 cells with a central hyperkalemic region, Wang and Rudy reported that a moderate increase ($[K^+]_o$=8.5 mM) increased SF and CV, whereas a more pronounced increase in $[K^+]_o$ (up to 13.5 mM) reduced SF[42] and conduction block occurred at $[K^+]_o$ > 14 mM.

With regard to the behavior of SF_R at the Purkinje-ventricle junction, our results show that an extensive uncoupling between Purkinje fibers and ventricular tissue, i.e. a high R_{PVJ}, can promote propagation failure in the junction (see Figure 1 panel C). However, an intermediate increase of ventricular cellular coupling restores propagation at this junction. Similar observations were made by Morley et al., who obtained aberrant propagation through PVJs in genetically modified mice.[43] Other theoretical studies have approached the evaluation of SF in a bundle of Purkinje fiber coupled to normal ventricular tissue,[21,44] but the present work quantifies for the first time propagation safety in the 1B ischemic ventricular tissue.

C Reentry in the Purkinje-Ventricle Subsystem

Under phase 1B ischemic conditions, UDBs and reentry in the Purkinje-ventricle interface were observed. The probability of occurrence increased for a low degree of uncoupling within the myocardium and at the PVJ. A critical temporal relationship between the worsening of ischemic conditions and uncoupling may be the origin of UDBs. Indeed, when $[K^+]_o$ accumulation is not high enough, conduction block does not occur, as can be inferred from the trend of the dark green region in Figure 1D-1F. In our 1D ring-shape and 2D models of the Purkinje-ventricle subsystem, propagation block occurred under 1B ischemia conditions at the PVJ1 and CIZ1B zones. Experiments focusing on action potential propagation from Purkinje fibers to ventricle have been performed on isolated cells,[45,46] and fiber preparations.[37,38,47] In a study conducted in Purkinje-ventricular cell pairs coupled with a variable resistance R_j, Huelsing et al. observed conduction block from Purkinje to ventricle at lower values of R_j than in the opposite direction.[46] They reported that uncoupling between

Purkinje and ventricular cells can enhance the likelihood of UDB. Additionally, Ferrier et al. observed bidirectional block in canine Purkinje fiber-papillary muscle preparations perfused with an ischemic solution.[48] Our simulations complement these reports by confirming the important role of uncoupling and ischemic components on conduction block in the Purkinje-ventricle subsystem.

Experimental and theoretical studies have also described reentry within ventricular tissue alone. Patterson and coworkers observed that during the period of 15-30 min of ischemia, ventricular extrasystoles were induced with conduction delays greater than 130 ms in canine mid-myocardial tissues.[2] They reported a relationship between delayed activation in the ischemic mid-myocardium and arrhythmias during phase 1B, and suggested that this aberrant impulse was generated by a localized reentry in ischemic mid-myocardium. On the other hand, Jie et al. confirmed with computer models that heterogeneous uncoupling resulted in dispersion of subepicardial effective refractory period, thus optimizing the substrate for reentry generation.[49]

In summary, we have further defined the conditions of phase 1B ischemia that can lead to conduction block in the Purkinje-ventricle subsystem and gained new insights into reentry generation in this setting. We observed that even a small degree of uncoupling between ventricular cells, as well as between Purkinje and ventricular tissue, may induce UDB and reentry in the Purkinje-ventricle subsystem. In contrast, a more extensive uncoupling can facilitate AP propagation. In the setting of phase 1B ischemia, the degree of hyperkalemia determines the range of uncoupling in which UDB may be induced. Additional experimental studies that analyze the effects of hyperkalemia and uncoupling (individually and combined) on reentry generation in the PVJ will be very valuable as a basis for improved understanding of arrhythmogenic mechanisms resulting from phase 1B ischemia.

Acknowledgements

References

1. van Rijen HV, de Bakker JM, van Veen TA. Hypoxia, electrical uncoupling, and conduction slowing: Role of conduction reserve. Cardiovasc Res. 2005;**66**:9-11.

2. Patterson E, Kalcich M, Scherlag BJ. Phase 1B ventricular arrhythmia in the dog: localized reentry within the mid-myocardium. J Interv Card Electrophysiol. 1998;**2**:145-61.

3. de Groot JR, Coronel R. Acute ischemia-induced gap junctional uncoupling and arrhythmogenesis. Cardiovasc Res. 2004;**62**:323-34.

4. Smith WT, Fleet WF, Johnson TA, Engle CL, Cascio WE. The Ib phase of ventricular arrhythmias in ischemic in situ porcine heart is related to changes in cell-to-cell electrical coupling. Experimental Cardiology Group, University of North Carolina. Circulation. 1995;**92**:3051-60.

5. Kaplinsky E, Ogawa S, Balke CW, Dreifus LS. Two periods of early ventricular arrhythmia in the canine acute myocardial infarction model. Circulation. 1979;**60**:397-403.

6. Cinca J, Warren M, Carreno A, Tresanchez M, Armadans L, Gomez P, et al. Changes in myocardial electrical impedance induced by coronary artery occlusion in pigs with and without preconditioning. Circulation. 1997;**96**:3079–3086.

7. Kleber AG, Riegger CB, Janse MJ. Electrical uncoupling and increase of extracellular resistance after induction of ischemia in isolated, arterially perfused rabbit papillary muscle. Circ Res. 1987;**61**:271–9.

8. de Groot JR, Wilms-Schopman FJ, Opthof T, Remme CA, Coronel R. Late ventricular arrhythmias during acute regional ischemia in the isolated blood perfused pig heart. Role of electrical cellular coupling. Cardiovasc Res. 2001;**50**:362-72.

9. Verkerk AO, Veldkamp MW, Coronel R, Wilders R, van Ginneken AC. Effects of cell-to-cell uncoupling and catecholamines on Purkinje and ventricular action potentials: implications for phase-1b arrhythmias. Cardiovasc Res. 2001;**51**:30-40.

10. Coronel R, Wilms-Schopman FJ, de Groot JR. Origin of ischemia induced phase 1b ventricular arrhythmias in pig hearts. J Am Coll Cardiol. 2002;**39**:166-76.

11. Coronel R,Wilms-Schopman FJ, Opthof T, Cinca J, Fiolet JW, Janse MJ. Reperfusion arrhythmias in isolated perfused pig hearts. Inhomogeneities in extracellular potassium, ST and TQ potentials, and transmembrane action potentials. Circ Res. 1992;**71**:1131-42.

12. Marzouk SA, Buck RP, Dunlap LA, Johnson TA, Cascio WE. Measurement of extracellular pH, K(+), and lactate in ischemic heart. Anal Biochem. 2002;**308**:52-60.

13. Faber GM, Rudy Y. Action potential and contractility changes in [Na(+)](i) overloaded cardiac myocytes: a simulation study. Biophys J. 2000;**78**:2392-404.

14. Viswanathan PC, Shaw RM, Rudy Y. Effects of IKr and IKs heterogeneity on action potential duration and its rate dependence: a simulation study. Circulation. 1999;**99**:2466-74.

15. Ferrero Jr JM, Saiz J, Ferrero JM, Thakor NV. Simulation of action potentials from metabolically impaired cardiac myocytes. Role of ATP-sensitive K+ current. Circ Res. 1996;**79**:208-21.

16. Ferrero Jr JM, Trenor B, Rodriguez B, Saiz J. Electrical activity and reentry during acute regional myocardial ischemia: insights from simulations. I J Bifurcation and Chaos. 2003;**13**:3703-3715.

17. Trenor B, Ferrero Jr JM, Rodriguez B, Montilla F. Effects of pinacidil on reentrant arrhythmias generated during acute regional ischemia: a simulation study. Ann Biomed Eng. 2005;**33**:897-906.

18. Trenor B, Romero L, Ferrero Jr JM, Saiz J, Molto G, Alonso JM. Vulnerability to reentry in a regionally ischemic tissue: a simulation study. Ann Biomed Eng. 2007;**35**:1756-70.

19. Stewart P, Aslanidi OV, Noble D, Noble PJ, Boyett MR, Zhang H. Mathematical models of the electrical action potential of Purkinje fibre cells. Philos Transact A Math Phys Eng Sci. 2009;**367**:2225-55.

20. Corrias A, Giles W, Rodriguez B. Ionic mechanisms of electrophysiological properties and repolarization abnormalities in rabbit Purkinje fibers. Am J Physiol Heart Circ Physiol. 2011;**300**:H1806-13.

21. Aslanidi OV, Stewart P, Boyett MR, Zhang H. Optimal velocity and safety of discontinuous conduction through the heterogeneous Purkinje-ventricular junction. Biophys J. 2009;**97**:20-39.

22. Li P, Rudy Y. A model of canine Purkinje cell electrophysiology and Ca2+ cycling: rate dependence, triggered activity, and comparison to ventricular myocytes. Circ Res. 2011;**109**:71-9.

23. Vaidyanathan R, O'Connell RP, Deo M, Milstein ML, Furspan P, Herron TJ, et al. The ionic bases of the action potential in isolated mouse cardiac Purkinje cell. Heart Rhythm. 2013;**10**:80-7.

24. Sampson KJ, Iyer V, Marks AR, Kass RS. A computational model of Purkinje fibre single cell electrophysiology: implications for the long QT syndrome. J Physiol. 2010;**588**:2643-55.

25. DiFrancesco D, Noble D. A model of cardiac electrical activity incorporating ionic pumps and concentration changes. Philos Trans R Soc Lond B Biol Sci. 1985;**307**:353-98.

26. Cabo C, Barr RC. Unidirectional block in a computer model of partially coupled segments of cardiac Purkinje tissue. Ann Biomed Eng. 1993;**21**:633-44.

27. Pollard AE, Cascio WE, Fast VG, Knisley SB. Modulation of triggered activity by uncoupling in the ischemic border. A model study with phase 1b-like conditions. Cardiovasc Res. 2002;**56**:381-92.

28. Jie X, Trayanova NA. Mechanisms for initiation of reentry in acute regional ischemia phase 1B. Heart Rhythm. 2010;**7**:379-86.

29. Wilensky RL, Tranum-Jensen J, Coronel R, Wilde AA, Fiolet JW, Janse MJ. The subendocardial border zone during acute ischemia of the rabbit heart: an electrophysiologic, metabolic, and morphologic correlative study. Circulation. 1986;**74**:1137-46.

30. Coronel R, Wilms-Schopman FJ, Fiolet JW, Opthof T, Janse MJ. The relation between extracellular potassium concentration and pH in the border zone during regional ischemia in isolated porcine hearts. J Mol Cell Cardiol. 1995;**27**:2069-73.

31. Coronel R, Fiolet JW, Wilms-Schopman FJ, Schaapherder AF, Johnson TA, Gettes LS, et al. Distribution of extracellular potassium and its relation to electrophysiologic changes during acute myocardial ischemia in the isolated perfused porcine heart. Circulation. 1988;**77**:1125-38.

32. Tan RC, Ramza BM, Joyner RW. Modulation of the Purkinje-ventricular muscle junctional conduction by elevated potassium and hypoxia. Circulation. 1989;**79**:1100–5.

33. Gilmour Jr RF, Evans JJ, Zipes DP. Purkinje-muscle coupling and endocardial response to hyperkalemia, hypoxia, and acidosis. Am J Physiol. 1984;**247**:H303–11.

34. Delgado C, Steinhaus B, Delmar M, Chialvo DR, Jalife J. Directional differences in excitability and margin of safety for propagation in sheep ventricular epicardial muscle. Circ Res. 1990;**67**:97–110.

35. Leon LJ, Roberge FA. Directional characteristics of action potential propagation in cardiac muscle. A model study. Circ Res. 1991;**69**:378-95.

36. Shaw RM, Rudy Y. Ionic mechanisms of propagation in cardiac tissue. Roles of the sodium and L-type calcium currents during reduced excitability and decreased gap junction coupling. Circ Res. 1997;**81**:727-41.

37. Romero L, Trenor B, Alonso JM, Tobon C, Saiz J, Ferrero Jr JM. The relative role of refractoriness and source-sink relationship in reentry generation during simulated acute ischemia. Ann Biomed Eng. 2009;**37**:1560–71.

38. de Groot JR. Genesis of life-threatening ventricular arrhythmias during the delayed phase of acute myocardial ischemia. Role of cellular electrical coupling and myocardial heterogeneities. University of Amsterdam; 2001.

39. Wilhelms M, Dossel O, Seemann G. Simulating the impact of the transmural extent of acute ischemia on the electrocardiogram. In: Computing in cardiology, 2010; 2010. p. 13-16.

40. del Rio CL, McConnell PI, Clymer BD, Dzwonczyk R, Michler RE, Billman GE, et al. Early time course of myocardial electrical impedance during acute coronary artery occlusion in pigs, dogs, and humans. J Appl Physiol. 2005;**99**:1576-81.

41. Dhein S. Cardiac ischemia and uncoupling: gap junctions in ischemia and infarction. Adv Cardiol. 2006;**42**:198-212.

42. Wang Y, Rudy Y. Action potential propagation in inhomogeneous cardiac tissue: safety factor considerations and ionic mechanism. Am J Physiol Heart Circ Physiol. 2000;**278**:H1019-H1029.

43. Morley GE, Danik SB, Bernstein S, Sun Y, Rosner G, Gutstein DE, et al. Reduced intercellular coupling leads to paradoxical propagation across the Purkinje-ventricular junction and aberrant myocardial activation. Proc Natl Acad Sci U S A. 2005;**102**:4126-9.

44. Boyle PM, Vigmond EJ. An intuitive safety factor for cardiac propagation. Biophys J. 2010;**98**:L57–9.

45. Huelsing DJ, Spitzer KW, Cordeiro JM, Pollard AE. Conduction between isolated rabbit Purkinje and ventricular myocytes coupled by a variable resistance. Am J Physiol. 1998;**274**:H1163-73.

46. Huelsing DJ, Spitzer KW, Pollard AE. Spontaneous activity induced in rabbit Purkinje myocytes during coupling to a depolarized model cell. Cardiovasc Res. 2003;**59**:620-7.

47. Evans JJ, Gilmour JRF, Zipes DP. The effects of lidocaine and quinidine on impulse propagation across the canine Purkinje-muscle junction during combined hyperkalemia, hypoxia, and acidosis. Circ Res. 1984;**55**:185-96.

48. Ferrier GR, Moffat MP, Lukas A. Possible mechanisms of ventricular arrhythmias elicited by ischemia followed by reperfusion. Studies on isolated canine ventricular tissues. Circ Res. 1985;**56**:184-94.

49. Jie X, Rodriguez B, de Groot JR, Coronel R, Trayanova N. Reentry in survived subepicardium coupled to depolarized and inexcitable midmyocardium: insights into arrhythmogenesis in ischemia phase 1B. Heart Rhythm. 2008;**5**:1036-44.

Tables

Table 1. Altered parameters in the model of phase 1B ischemia. These include: the ventricular tissue resistance (R_{endo}), intracellular sodium concentration ($[Na^+]_i$), extracellular potassium concentration ($[K^+]_o$), the parameters involved in the sarcoplasmic reticulum calcium dynamics ($G_{rel,CICR}$, $G_{rel, ov}$ and $I_{up, bar}$), the parameters for specific Ca^{2+} currents ($G_{Ca, L}$, $G_{Ca, b}$ and $P_{ns, Ca}$), a constant related to sodium-calcium exchanger current ($C_{1, NCX}$), a constant related to sodium-sodium pump ($I_{NaK, bar}$), the intracellular ADP concentration ($[ADP]_i$), and the intracellular ATP concentration ($[ATP]_i$). Note that all parameters remain unchanged in the 1B central ischemic zone (CIZ1B) and in the normal ventricular zone (NZ). However, the 13 parameters assumed to be altered by phase 1B ischemia conditions were altered to reflect a spatial gradient in the border zone (BZ).

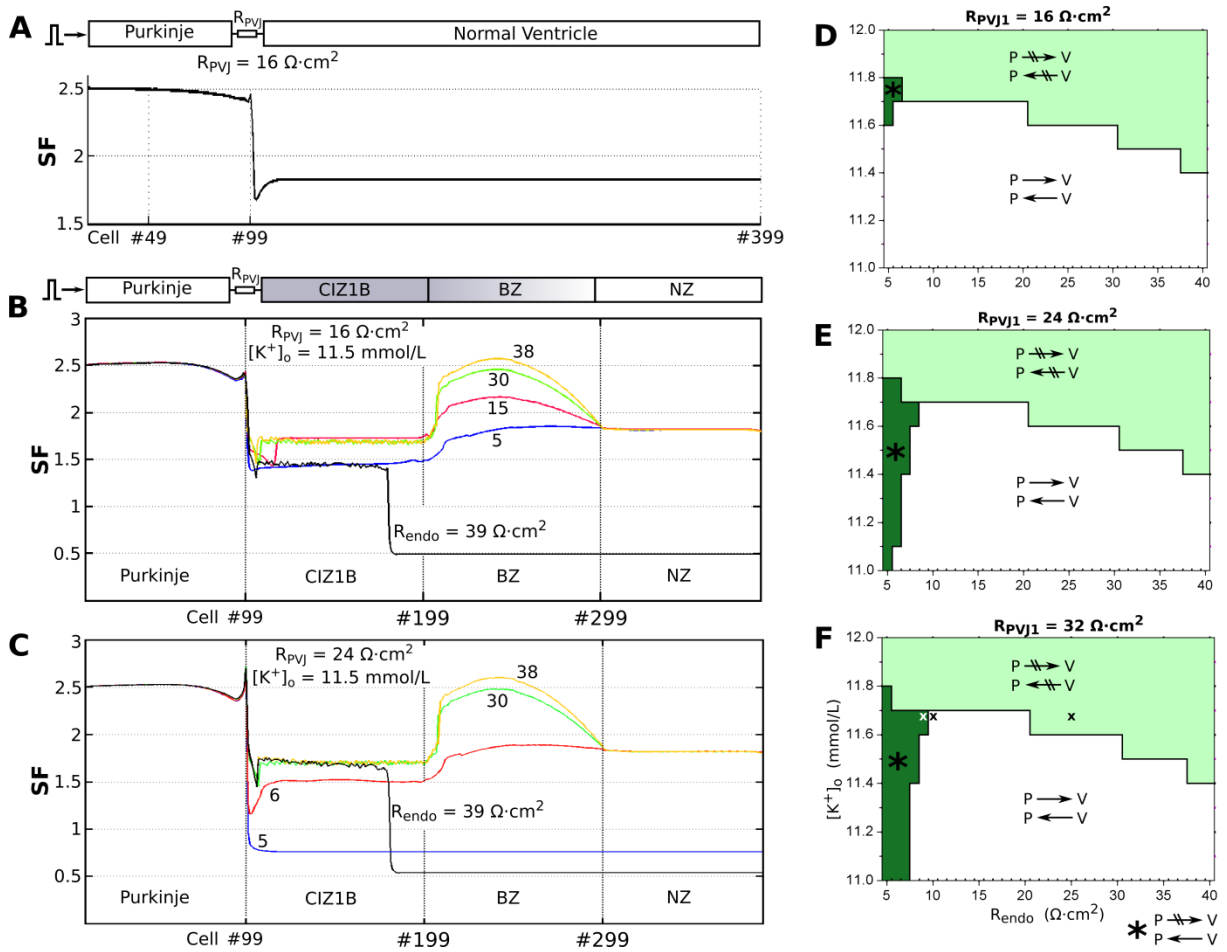| Parameter	Value in NZ	Value in CIZ1B	Width of the BZ (mm)
$R_{endo}(\Omega \cdot cm^2)$	5	5 - 40	100
$[K^+]_o(mM)$	5.4	5.4 -12	100
$[Na^+]_i(mM)$	10	15	100
$[ATP]_i(mM)$	6.8	3.8	10
$[ADP]_i(mM)$	15	110	10
$C_{1, NCX}$ (mA/mF)	$2.5 \cdot 10^{-4}$	$1.625 \cdot 10^{-4}$	100
$G_{Ca, b}(mS/mF)$	$3.016 \cdot 10^{-3}$	$4.11 \cdot 10^{-3}$	10
$G_{rel,CICR}$ (ms^{-1})	150	7.5	100
$G_{rel, ov}$ (ms^{-1})	4	2.6	100
$I_{NaK, bar}$ (mA/mF)	2.25	$4.5 \cdot 10^{-1}$	10
$I_{up, bar}$ (mM·ms)	$8.75 \cdot 10^{-3}$	$4.5 \cdot 10^{-3}$	100
$P_{Ca, L}(cm/s)$	$5.4 \cdot 10^{-4}$	$2.7 \cdot 10^{-4}$	50
$P_{ns, Ca}(cm/s)$	$1.75 \cdot 10^{-7}$	$2.98 \cdot 10^{-7}$	10

Figures

Fig. 1. Safety factor calculated along the Purkinje and ventricular fibers. **A**. SF_R in the Purkinje fiber coupled to the ventricular fiber under normal conditions. **B and C**. SF_R obtained in the Purkinje fiber coupled to the ventricular fiber under phase 1B ischemia conditions. Various combinations of coupling between both fibers (R_{PVJ}), of $[K^+]_o$, and cellular coupling between endocardial cells (R_{endo}) were considered in the simulations. **D, E and F.** Simulations of AP propagation and block as a function of ventricular cellular coupling (R_{endo}), $[K^+]_o$ and Purkinje-ventricle resistance (R_{PVJ}). A 1D model of the Purkinje fiber (100 cells) connected to the ischemic ventricular fiber (300 cells) was used. Stimuli were applied at cell #0 of the Purkinje fiber or at cell #399 of the ventricular fiber. The white area represents the cases where AP propagation from Purkinje to ventricle and from ventricle to Purkinje was observed. The light green area represents the cases of AP conduction block from Purkinje to ventricle and from ventricle to Purkinje (bidirectional conduction block, BDB). The dark green areas represent the cases of conduction block from Purkinje to ventricle and AP conduction from ventricle to Purkinje (unidirectional conduction block, UDB). Three crosses are depicted in panel F to indicate three scenarios considered in Figure 2.
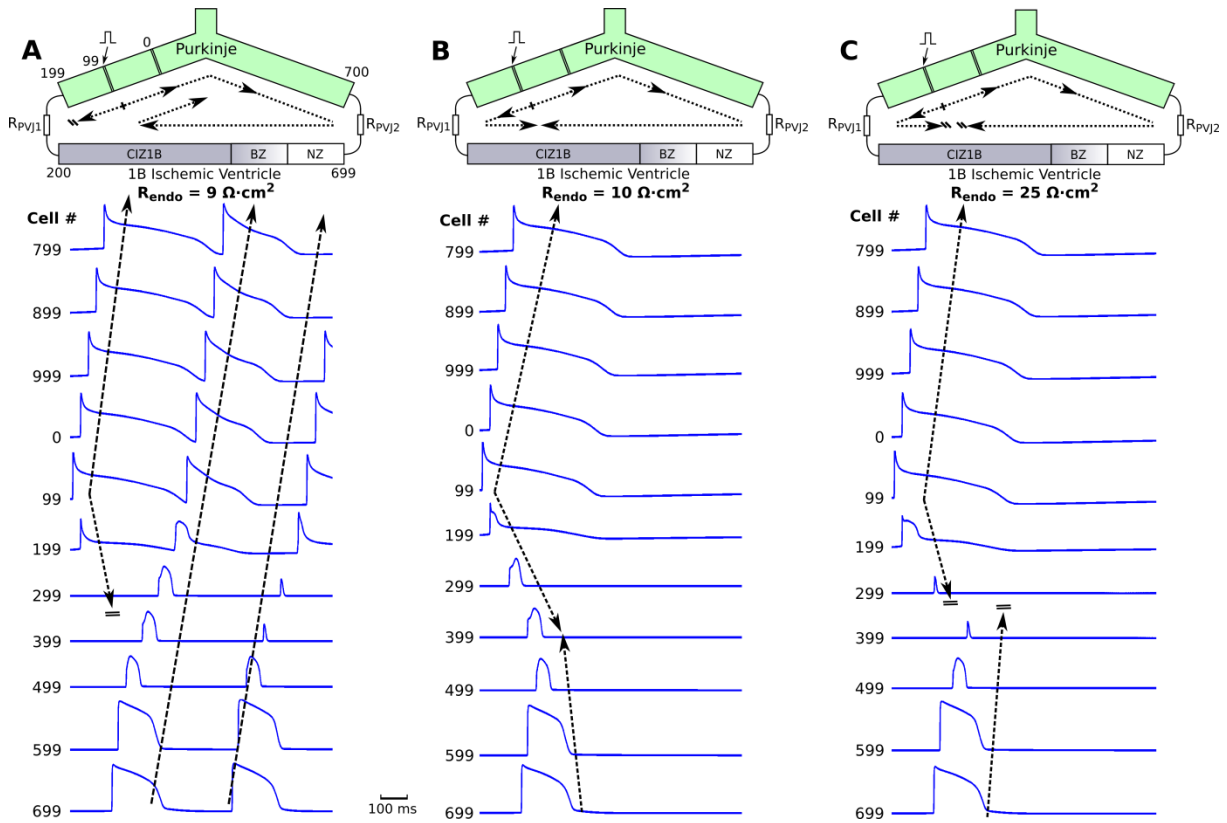
Fig. 2. Reentry, collision and bidirectional block (BDB) (from left to right) observed in a virtual 1D ring composed of a Purkinje fiber coupled to a phase 1Bischemic ventricular fiber through two Purkinje-ventricle junctions. Uncoupling within the ischemic zone (R_{endo}) was increased progressing from panel **A** through panel **C**. Two stimuli at a basic cycle length of 1500 ms were applied to cell #99 of the Purkinje fiber. The APs generated by the second pulse are shown for the indicated cells. $[K^+]_o$ was set to 11.7 mM and R_{PVJ1} and R_{PVJ2} were set to 32 and 16 $\Omega \cdot cm^2$, respectively.
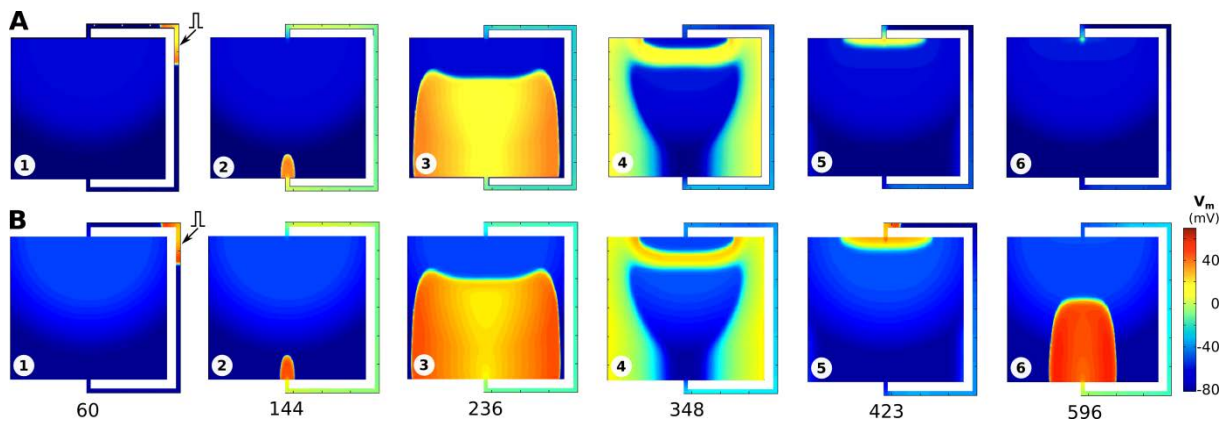

Fig. 3. Voltage profiles at selected simulation time points utilizing a two-dimensional model consisting of a bundle of Purkinje fibers coupled to a sheet of 1B ischemic ventricular tissue. **A.** Bidirectional conduction block at PVJ1 junction when $[K^+]_o$=14.3 mM. **B.** Reentry in the presence of $[K^+]_o$ = 14.5 mM.